

Measurement and DFT Calculation of $\text{Fe}(\text{cp})_2$ Redox Potential in Molecular Monolayers Covalently Bound to H–Si(100)

M. Cossi,^{*,†} M. F. Iozzi,[†] A. G. Marrani,[‡] T. Lavecchia,[‡] P. Galloni,[‡] R. Zanoni,[‡] and F. Decker[‡]

Dipartimento di Chimica, Università degli Studi di Napoli “Federico II”, Complesso Monte S. Angelo, 80126 Naples, Italy, and Dipartimento di Chimica, Università degli Studi di Roma “La Sapienza”, p.le Aldo Moro 5, 00185 Rome, Italy

Received: July 27, 2006; In Final Form: September 15, 2006

The electron transfer to self-assembled molecular monolayers carrying a ferrocene (Fc) center, grafted on a flat Si(100) surface, is a recent subject of experimental investigation. We report here the density functional theory (DFT) *ab initio* calculation of Fc–silicon hybrid redox potentials. The systems were modeled with a slab of H-terminated Si(100) 1×1 and 2×1 surfaces: geometries were optimized using the ONIOM method, and solute–solvent interactions were included through the polarizable continuum model (PCM) method. Two new routes for Si functionalization with ethyl– (EtFc) and ethynyl–Fc (EFC) differing only in the unsaturation degree of the anchoring arm have been successfully explored, and the redox potential of the resulting hybrids has been measured by cyclic voltammetry: 0.675 and 0.851 V versus NHE for the EtFc and EFC derivatives, respectively. These values, along with the previously measured potential (0.700 V) for the mono-unsaturated derivative, vinyl–Fc, allow the relation between the unsaturation degree and the adduct redox potential to be studied. The comparison among the measured and computed potentials allows one to discriminate between different adduct isomers for the saturated species and more importantly provides strong indications that the carbon–carbon unsaturation initially present in the molecular arm used for anchoring to the surface is preserved upon addition, in contrast with the commonly accepted reaction mechanism.

1. Introduction

Self-assembled, redox-active organic monolayers on Si electrodes constitute a promising step toward molecule-based hybrid devices compatible with the crystalline silicon platforms like FLASH and DRAM memories¹ or chemical/biological sensors.^{2–4} Due to the attractive electrochemical properties of ferrocenes (fast e-transfer rates and favorable redox potentials), their introduction in organic monolayers bound to gold has been widely described in the literature.^{5–10} So far, however, the anchoring of ferrocene (Fc) derivatives on Si has been seldom attempted, maybe due to the difficulty of establishing robust Si–C or Si–O bonds without oxidation of the Si substrate. Fc substituted by short linkers anchored directly on Si(100)^{11–16} or coupled to preassembled, acid-terminated alkyl monolayers on Si(111) have recently been reported.¹⁷ Although a meaningful comparison of the former with the latter approach is difficult, due to the inherently different reactivities of the (100) and (111) surfaces, it was found that the short-chain redox hybrids on Si(100) have higher e-transfer rates but shorter lifetimes than the mixed Fc–alkyl layers on Si(111).¹¹

The chemical route mostly used to establish a carbosilane bond between Si and the redox organometallic molecules has

been the reaction of unsaturated molecular linkers with the H-terminated Si(100) or (111) surfaces, activated by visible or UV radiation.¹⁸ The proposed mechanisms are different: the UV-induced hydrosilylation involves photolytic homolysis of a surface Si–H bond, giving rise to a radical chain reaction;¹² visible-light activation is believed to proceed via a surface exciton, in photoluminescent nanocrystalline silicon,^{19,20} while for flat Si the role of the exciton has been tentatively rephrased in terms of surface plasmons.²¹

The hybrids obtained with visible-light activation bear an unknown degree of unsaturation in the C–C tethering arm, which is assumed to be reduced (from triple to double and from double to single C–C bond) upon the reaction. The anchoring on Si of a fully saturated C–C chain with a redox head, although desirable, has not been shown so far. Conversely, reaction routes allowing a controlled unsaturation in the molecules in the self-assembled monolayer (SAM) to be maintained have not been explored to a large extent.

In order to reach extramild conditions for attachment to Si, we have successfully tested the visible-light photostimulated reaction of ethylferrocene on H–Si. Such a reaction of a saturated hydrocarbon arm was never reported previously: the possible mechanisms, which are being investigated by accurate *ab initio* calculations, are beyond the scope of this Letter and will be discussed in a further work. We anticipate that the reaction profiles, and hence the potential energy barriers, are strongly dependent on the electronic state of the inorganic

* To whom correspondence should be addressed. E-mail: maurizio.cossi@unina.it.

[†] Università degli Studi di Napoli “Federico II”.

[‡] Università degli Studi di Roma “La Sapienza”.

cluster, as already shown for a different reaction in ref 22, indicating that the suitable surface exciton can favor the present reaction with respect to other hydrosilylation mechanisms which require the reduction of unsaturated bonds.

We have observed from cyclic voltammograms that the redox potential of the series ethyl-Fc, vinyl-Fc, and ethynyl-Fc in acetonitrile solution increases with the unsaturation degree of the C–C terminal bond and found an excellent agreement with the potentials computed theoretically. Then, we have developed suitable grafting procedures to yield the corresponding series of redox molecular hybrids on Si: with a combined experimental/theoretical approach, the hybrid redox potentials were measured by cyclic voltammetry and computed with accurate quantum mechanical procedures. The very satisfactory match of theoretical and experimental results shows that this procedure can be confidently used to test for the presence of unsaturated bonds in the grafted redox monolayers.

2. Experimental Procedures and Results

The functionalization experiments on the surface-activated samples were carried out using standard preparative Schlenk-line procedures. Ethylferrocene (EtFC), 97% ethynylferrocene (EFC), 1.6 M butyllithium solution in hexane, 99% trifluoroacetic acid (purchased from Aldrich), and dry diethyl ether over molecular sieves (purchased from Fluka) were used as received. Dichloromethane (purchased from Fluka) was dried by distillation over CaH_2 under N_2 . Single-side polished Si(100) wafers (from Si-Mat), about 0.35 mm thick, p-doped ($0.02 \Omega \text{ cm}$ resistivity) with areas of $\sim 1 \text{ cm}^2$, were cleaned and hydrogenated following a procedure we recently reported.²³ Several functionalized Si samples were prepared following two different routes on freshly etched Si substrates. An extramild white-light-activated grafting and cleaning procedure described in our recent reports for vinylferrocene (VFC)¹¹ was used for the reaction between ethylferrocene (liquid at r.t.) and H-terminated Si. In the case of EFC, a procedure reported in the literature,²⁴ for the synthesis of lithium ferrocenylethynylide, was adapted to Si functionalization. The desired hybrid was produced by adding the freshly etched Si sample to a solution of lithium ferrocenylethynylide in diethyl ether and allowing them to react for 15 h at room temperature. After functionalization, the Si samples were cleaned thoroughly with an acidic solution (1% TFA in Et_2O) and rinsed with different solvents (CH_2Cl_2 , Et_2O) in an ultrasonic bath. These two routes for Si functionalization are unprecedented, and details about the procedures will be reported elsewhere. Following the same procedure applied to VFC monolayers,¹¹ the EtFC and EFC SAMs were characterized by atomic force microscopy (AFM) and X-ray photoelectron spectroscopy (XPS), proving the presence of Fe(II) with a minor amount of Fe(III), both related to the ferrocene moieties anchored to the surface, the near absence of Si oxides (SiO_x), and the establishment of a Si–C bond (see the XPS spectra in the Supporting Information). After monolayer formation, Ohmic contact to Si was made according to ref 23 and the Si crystal was pressed against an O-ring sealing a small aperture in the PTFE cell, defining exactly the electrode area (0.3 cm^2). The electrochemical properties of the ferrocene derivative monolayers covalently bound to p-Si(100) surfaces were explored mainly by cyclic voltammetry in 0.1 M NEt_4ClO_4 (TEAP) in dry CH_3CN containing no deliberately added electroactive species.

Representative cyclic voltammograms (cv's) of p-Si(100) electrodes functionalized with ethylferrocene (EtFC/p-Si) and ethynylferrocene (EFC/p-Si) in $\text{CH}_3\text{CN}/\text{TEAP}$ (0.1 M) are

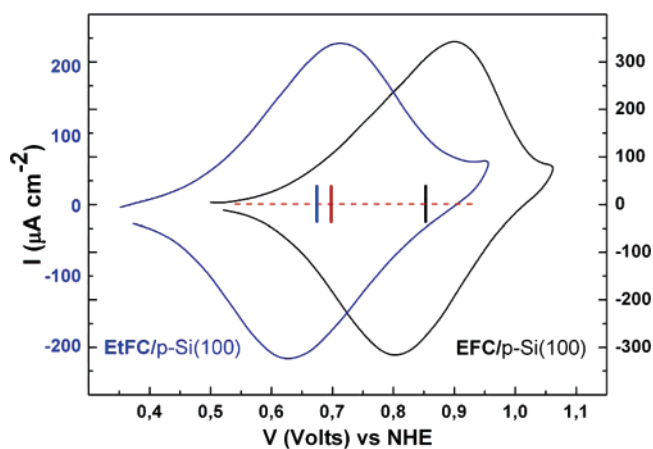


Figure 1. Cyclic voltammograms taken at 10 V s^{-1} of the saturated hybrid (p-Si- CH_2CH_2 -Fc), blue curve, left current scale, and of the doubly unsaturated hybrid (p-Si- CC -Fc), black curve, right current scale, in $\text{CH}_3\text{CN}/\text{TEAP}$ (0.1 M). The vertical bars indicate the redox potential of both samples, together with that for vinyl-ferrocene (0.7 V for p-Si- CHCH -Fc), as reported in ref 23.

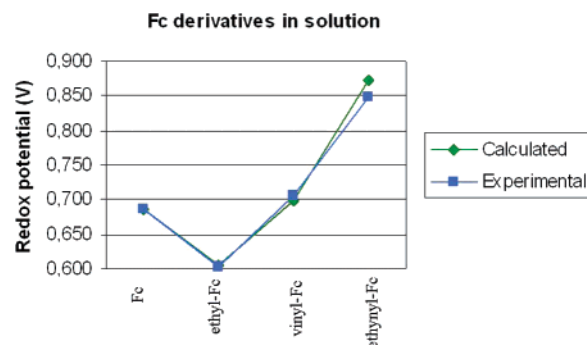


Figure 2. Computed and experimental redox potential (volts, referred to NHE) for Fc derivatives in acetonitrile.

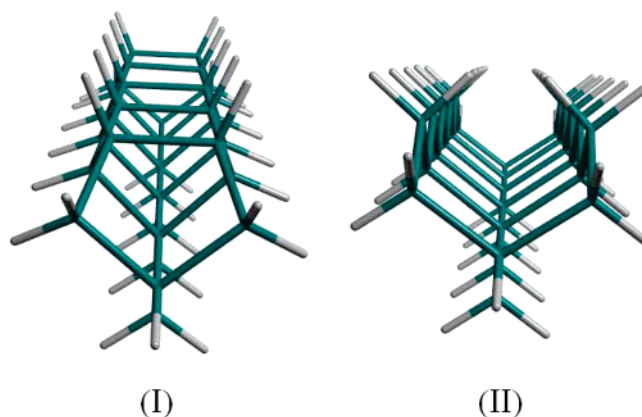


Figure 3. Si_3H_{38} (I) and Si_3H_{48} (II) clusters modeling the Si-2 \times 1 and Si-1 \times 1 surfaces, respectively.

shown in Figure 1. The electrode potential was scanned from the lower to the higher limit and back at 10 V/s , inducing the reversible oxidation of $\text{Fe}(\text{cp})_2$ derivative groups. The E° value, estimated from the mean of the anodic and cathodic peak potentials, was 0.675 V versus NHE for EtFC/p-Si and 0.851 V versus NHE for EFC/p-Si. In both cases, the dependence of the peak current on the scan rate was linear, indicating a surface-controlled redox process (see data in the Supporting Information). The analysis²⁵ of the area under the voltammetric peaks yielded surface coverage values of 2.4×10^{-11} and $3.1 \times 10^{-11} \text{ mol cm}^{-2}$ for the EtFC and EFC/p-Si hybrids, respectively. The values of the peak widths at half-maximum (ΔE_{fwhm}) were 190

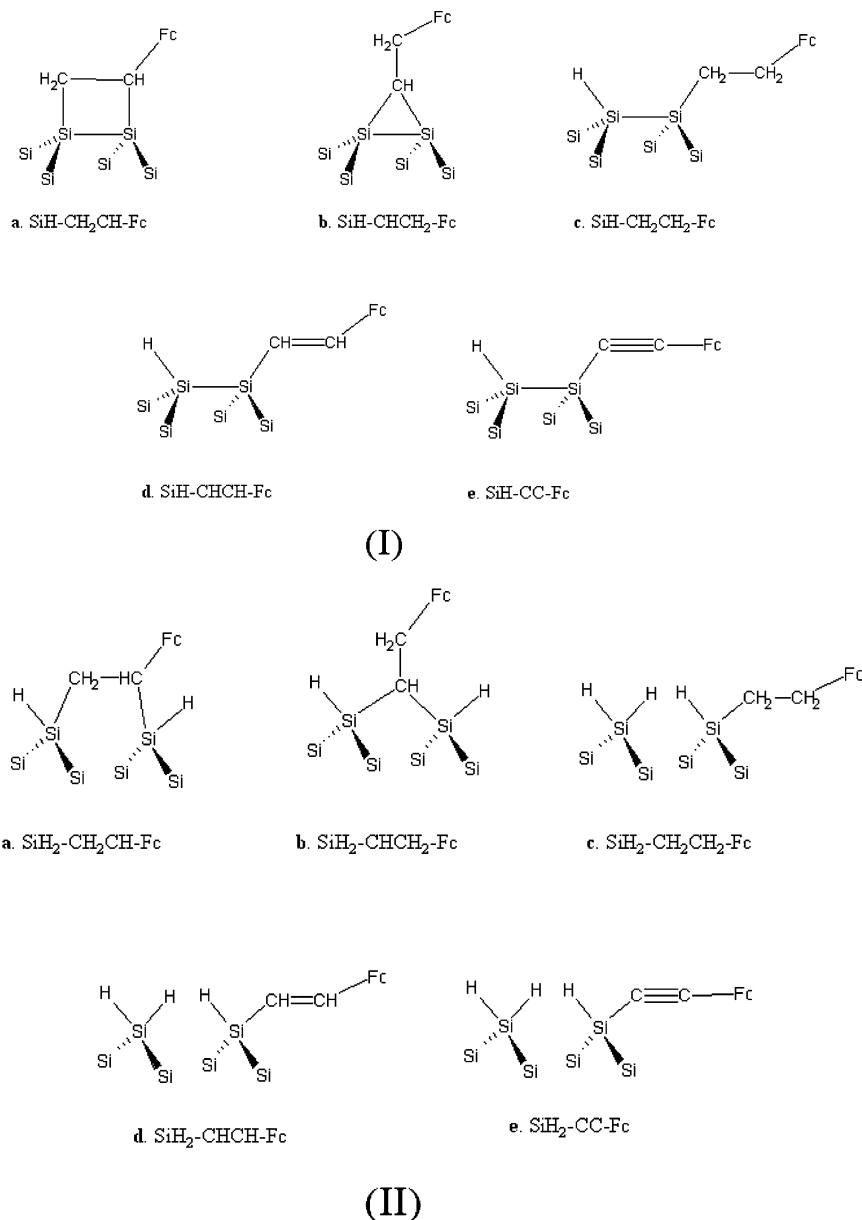


Figure 4. Structures of ethyl-, vinyl-, and ethynyl-Fc adsorbed on mono-hydrogenated (I) and di-hydrogenated (II) silicon surfaces.

and 200 mV at 10 V/s for the EtFC and EFC monolayers, respectively, larger than the theoretical (entropically determined) value of 91 mV, expected for identical, independent redox sites at room temperature²⁵ but narrow enough for unambiguous peak resolution. The broadness of the cv waves can be interpreted as evidence for substantial repulsive interactions between nearest neighboring ferrocenyl groups on the surface.²⁶ The peak-to-peak separation (ΔE_{pp}) was 62 mV at 10 V/s, for the EtFC monolayer, and 74 mV at the same scan rate, for the EFC analogue. These values differ from the zero peak-to-peak separation, theoretically predicted for an ideal surface-confined redox couple,²⁷ and indicate that the scan rate is comparable to the electron transfer rate, at the higher sweep speeds. From the peak-to-peak separation values in these cv's, standard electron transfer rate constants (k_0) (i.e., the rate constant corresponding to electron self-exchange under conditions where the reaction driving force is zero) were obtained with Laviron's approach for electroactive species immobilized onto an electrode surface.²⁷ From this analysis of the cv's, the electron transfer rate constants were 202 and 164 s⁻¹ ($\pm 10\%$), for the EtFC and EFC/p-Si hybrids, respectively, slightly higher than the values found for

vinylferrocene (VFC/p-Si), our reference system for monolayer quality on Si(100).²⁸

3. Theoretical Results and Comparison With Measured Potentials

Redox potentials (in volts) are theoretically evaluated by computing the molecular energies for the oxidized and reduced forms in the suitable solvent (acetonitrile in our case):²⁹

$$V = -[(E_{\text{red}} - E_{\text{ox}}) + (\Delta G_{\text{red}}^{\text{CH}_3\text{CN}} - \Delta G_{\text{ox}}^{\text{CH}_3\text{CN}})] - V^0 \quad (1)$$

where the energies (E_x) (conventionally more negative for stabler species) and the solvation free energies ($\Delta G_x^{\text{CH}_3\text{CN}}$) are computed in electronvolts at the theory level specified below and V^0 is the absolute potential of the reference electrode; for instance, the normal hydrogen electrode (NHE), to which the following calculations are referred, has $V^0 = 4.43$ V.³⁰ The computed potentials can be directly compared to the experimental ones, provided the latter are referred to the same standard electrode. We did not include thermal (vibrational and rotational)

contributions, whose variations among the substituted ferrocenes are assumed to be negligible, as confirmed by the very good agreement with the experimental potentials of the ferrocene derivatives in solution (see Figure 2 below).

The density functional theory (DFT) was used, with the B3LYP functional³¹ and a large Gaussian basis set, that is, 6-31+G(d,p),^{32,33} for the second row atoms, LANL2DZ effective core potentials and basis set³⁴ for Si, and LANL2DZ with 3 *f* and 1 *g* polarization functions for Fe. The same basis set was used for both geometry optimizations and potential calculations on the isolated Fc derivatives.

The solute–solvent interactions were included through the polarizable continuum model (PCM).^{35,36} In this method, the solute is accommodated in a cavity, formed by spheres centered on the solute atoms, and the solvent reaction field is described in terms of apparent charges on the cavity walls. Starting from a widely used compilation of atomic radii,³⁷ optimized for aqueous solutions, we adjusted the radii for the present solvent, that is, acetonitrile. The cavity for the isolated Fc was scaled, in order to reproduce the experimental redox potential in acetonitrile through eq 1: the same scaling factor was successfully applied to the carbon atomic spheres in all of the Fc derivatives, without any further adjustment.

The computed and experimental potentials for Fc and Fc derivatives in acetonitrile are shown in Figure 2: though the PCM cavity was optimized only for Fc, excellent agreement is found for all of the species.

For the Fc–silicon adducts, the inorganic moiety was modeled with Si₃₃H₃₈ and Si₃₃H₄₈ clusters reproducing a portion of the hydrogenated (100) surface, with 2 × 1 and 1 × 1 reconstructions, respectively (in the two structures, the surface Si dimers are mono- and di-hydrogenated, respectively, see Figure 3).

The adduct geometries were optimized using the ONIOM method,³⁸ in which the system is divided into two parts, studied with different theoretical approaches: the Fc and the bound silicon atom were treated at the DFT level, while for the rest of the cluster the semiempirical MSINDO method³⁹ was used. Different adduct structures were optimized, both on the Si-2 × 1 and on the Si-1 × 1 surfaces, as sketched in Figure 4.

On these structures, the redox potential was computed at the DFT/B3LYP level with the complete basis set cited above, extending the ab initio calculation to the whole Fc–silicon adduct; for the calculation of solvent effects, the whole adduct was embedded in the solute cavity, and the same PCM parameters as above were used, leaving the default sphere for silicon.

The computed potentials for the adducts on Si-2 × 1 and Si-1 × 1 are reported in Figure 5, along with the experimental values obtained for the adducts with EtFC, VFC, and EFC.

The agreement is less satisfactory than that for isolated Fc's, probably due to the use of standard spheres for Si in the PCM cavities. In any case, the measured potential for the adduct obtained from EtFC (whose carbon chain is surely saturated) is clearly more compatible with structure c.

Even within the systematic theoretical error, the comparison of calculated and measured potentials for the VFC and EFC adducts seems to indicate that the carbon chain unsaturations are preserved upon adsorption, in contrast with the common interpretation of the addition mechanism. This conclusion is reinforced by considering the differences among the measured potentials and among the computed values for structures c, d, and e (i.e., by assuming that the systematic error is the same for saturated and unsaturated adducts).

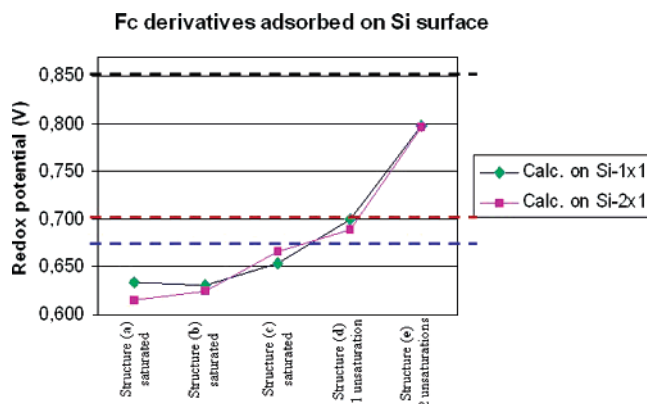


Figure 5. Computed redox potential (volts, referred to NHE) for different Fc derivative adducts on mono- and di-hydrogenated silicon surfaces. The experimental values for the adducts obtained with ethyl- (blue), vinyl- (red), and ethynyl-Fc (black) are also reported for comparison.

4. Conclusions

Two new routes for the functionalization of the Si(100) surface with saturated and doubly unsaturated ferrocene alkyl derivatives were developed, and the redox potential of the resulting molecular layers was measured by cyclic voltammetry. The redox potentials of isolated and adsorbed ferrocene derivatives were also computed theoretically at the DFT level, with inclusion of the solvent effects: excellent agreement with the experimental potentials was found for the isolated species.

Comparing the computed and measured potentials for the adducts with different unsaturation degrees in the C–C anchoring arm, we could discriminate between different isomers of the saturated adduct, and we found strong indications that the unsaturations are preserved during the addition, thus suggesting that the hydrosilylation activated by visible light proceeds through a mechanism not yet described.

Acknowledgment. The financial support of MUIR, Ministero dell'Università e Ricerca (COFIN 2004, COFIN 2005) is gratefully acknowledged.

Supporting Information Available: Figures showing anodic and cathodic peak current densities for EtFC/p-Si and EFC/p-Si, XPS spectra of EtFC/p-Si taken from the Si 2p and Fe 2p regions, and XPS spectra of EFC/p-Si taken from the Si 2p and Fe 2p regions. This material is available free of charge via the Internet at <http://pubs.acs.org>.

References and Notes

- (1) Roth, K. R.; Yasserli, A. A.; Liu, Z.; Dabke, R. B.; Malinovskii, V.; Schweikart, K. H.; Yu, L.; Tiznado, H.; Zaera, F.; Lindsey, J. S.; Kuhr, W. G.; Bocian, D. F. *J. Am. Chem. Soc.* **2003**, *125*, 505.
- (2) Buriak, J. M. *Chem. Rev.* **2002**, *102*, 1271.
- (3) Wayner, D. D. M.; Wolkow, R. A. *J. Chem. Soc., Perkin Trans.* **2002**, *2*, 23.
- (4) Bent, S. F. *J. Phys. Chem. B* **2002**, *106*, 2830.
- (5) Chidsey, C. E. D.; Bertozzi, C. R.; Putvinski, T. M.; Muijsce, A. M. *J. Am. Chem. Soc.* **1990**, *112*, 4301.
- (6) Chidsey, C. E. D. *Science* **1991**, *251*, 919.
- (7) Smalley, J. F.; Sachs, S. B.; Chidsey, C. E. D.; Dudek, S. P.; Sikes, H. D.; Creager, S. E.; Yu, C. J.; Feldberg, S. W.; Newton, M. D. *J. Am. Chem. Soc.* **2004**, *126*, 14620.
- (8) Sikes, H. D.; Smalley, J. F.; Dudek, S. P.; Cook, A. R.; Newton, M. D.; Chidsey, C. E. D.; Feldberg, S. W. *Science* **2001**, *291*, 1519.
- (9) Sachs, S. B.; Dudek, S. P.; Hsung, R. P.; Sita, L. R.; Smalley, J. F.; Newton, M. D.; Feldberg, S. W.; Chidsey, C. E. D. *J. Am. Chem. Soc.* **1997**, *119*, 10563.

- (10) Creager, S.; Yu, C. J.; Bambad, C.; O'Connor, S.; MacLean, T.; Lam, E.; Chong, Y.; Olsen, G. T.; Luo, J.; Gozin, M.; Kayyem, J. F. *J. Am. Chem. Soc.* **1999**, *121*, 1059.
- (11) Dalchiale, E. A.; Aurora, A.; Bernardini, G.; Cattaruzza, F.; Flamini, A.; Pallavicini, P.; Zanon, R.; Decker, F. *J. Electroanal. Chem.* **2005**, *579*, 133.
- (12) Kruse, P.; Johnson, E. R.; DiLabio, G. A.; Wolkow, R. A. *Nano Lett.* **2002**, *2*, 807.
- (13) Li, Q.; Mathur, G.; Gowda, S.; Surthi, S.; Zhao, Q.; Yu, L.; Lindsey, J. S.; Bocian, D. F.; Misra, V. *Adv. Mater.* **2004**, *16*, 133.
- (14) Balakumar, A.; Lysenko, A. B.; Carcel, C.; Malinovskii, V. L.; Gryko, D. T.; Schweikart, K. H.; Loewe, L. S.; Yasseri, A. A.; Liu, Z.; Bocian, D. F.; Lindsey, J. S. *J. Org. Chem.* **2004**, *69*, 1435.
- (15) Roth, K. M.; Yasseri, A. A.; Liu, Z.; Dabke, R. B.; Malinovskii, V.; Schweikart, K.-H.; Yu, L.; Tiznado, H.; Zaera, F.; Lindsey, J. S.; Kuhr, W. G.; Bocian, D. F. *J. Am. Chem. Soc.* **2003**, *125*, 505.
- (16) Li, Q.; Mathur, G.; Homs, M.; Surthi, S.; Misra, V.; Malinovskii, V.; Schweikart, K.-H.; Yu, L.; Lindsey, J. S.; Liu, Z.; Dabke, R. B.; Yasseri, A.; Bocian, D. F.; Kuhr, W. G. *Appl. Phys. Lett.* **2002**, *81*, 1494.
- (17) Fabre, B.; Hauquier, F. *J. Phys. Chem. B* **2006**, *110*, 6848.
- (18) Buriak, J. M. *Chem. Commun.* **1999**, *99*, 1051.
- (19) Stewart, M. P.; Buriak, J. M. *J. Am. Chem. Soc.* **2001**, *123*, 7821.
- (20) Schmeltzer, J. M.; Porter, L. A.; Stewart, M. P.; Buriak, J. M. *Langmuir* **2002**, *18*, 2971.
- (21) Sun, Q.-Y.; Louis, de Smet, C. P. M.; van Lagen, B.; Wright, A.; Zuilhof, H.; Sudhoefer, E. J. R. *Angew. Chem., Int. Ed.* **2004**, *43*, 1352.
- (22) Reboredo, F. A.; Schwengler, E.; Galli, G. *J. Am. Chem. Soc.* **2003**, *125*, 15243.
- (23) Zanon, R.; Cattaruzza, F.; Coluzza, C.; Dalchiale, E. A.; Decker, F.; Di Santo, G.; Flamini, A.; Funari, L.; Marrani, A. G. *Surf. Sci.* **2005**, *575*, 260.
- (24) Kuo, C.-K.; Chang, J.-C.; Yeh, C.-Y.; Lee, G.-H.; Wang, C.-C.; Peng, S.-M. *Dalton Trans.* **2005**, 3696.
- (25) Finklea, H. O. In *Encyclopedia of Analytical Chemistry*; Meyers, R. A., Ed.; John Wiley and Sons Ltd.: Chichester, U.K., 2000; pp 1–26.
- (26) Eagling, R. D.; Bateman, J. E.; Goodwin, N. J.; Henderson, W.; Horrocks, B. R.; Houlton, A. *J. Chem. Soc., Dalton Trans.* **1998**, 1273.
- (27) Laviron, E. *J. Electroanal. Chem.* **1979**, *101*, 19.
- (28) Decker, F.; Cattaruzza, F.; Coluzza, C.; Flamini, A.; Marrani, A. G.; Zanon, R.; Dalchiale, E. A. *J. Phys. Chem. B* **2006**, *110*, 7374.
- (29) (a) Winget, P.; Weber, E. J.; Cramer, C. J.; Truhlar, D. G. *Phys. Chem. Chem. Phys.* **2000**, 1931. (b) Fu, Y.; Liu, L.; Yu, H.-Z.; Wang, Y.-M.; Guo, Q.-X. *J. Am. Chem. Soc.* **2005**, *127*, 7227.
- (30) Reiss, H.; Heller, A. *J. Phys. Chem.* **1985**, *89*, 4207.
- (31) Becke, A. D. *Phys. Rev. B* **1988**, *38*, 3098.
- (32) Dunning, T. H., Jr. *J. Chem. Phys.* **1989**, *90*, 1007.
- (33) Petersson, G. A.; Al-Laham, M. A. *J. Chem. Phys.* **1991**, *94*, 6081.
- (34) (a) Hay, P. J.; Wadt, W. R. *J. Chem. Phys.* **1982**, *82*, 270. (b) Wadt, W. R.; Hay, P. J. *J. Chem. Phys.* **1985**, *82*, 284. (c) Hay, P. J.; Wadt, W. R. *J. Chem. Phys.* **1985**, *82*, 299.
- (35) Vreven, T.; Morokuma, K.; Farkas, O.; Schlegel, H. B.; Frisch, M. J. *J. Comput. Chem.* **2003**, *24*, 760.
- (36) (a) Ahlswede, B.; Jug, K. *J. Comput. Chem.* **1999**, *20*, 563. (b) Ahlswede, B.; Jug, K. *J. Comput. Chem.* **1999**, *20*, 572. (c) Bredow, T.; Geudtner, G.; Jug, K. *J. Comput. Chem.* **2001**, *22*, 861.
- (37) Miertus, S.; Scrocco, E.; Tomasi, J. *Chem. Phys.* **1981**, *55*, 117.
- (38) Cossi, M.; Rega, N.; Scalmani, G.; Barone, V. *J. Comput. Chem.* **2003**, *24*, 669.
- (39) Barone, V.; Cossi, M.; Tomasi, J. *J. Chem. Phys.* **1997**, *107*, 3210.